

Cite this: *J. Mater. Chem.*, 2012, **22**, 25354

www.rsc.org/materials

PAPER

A facile preparation of targetable pH-sensitive polymeric nanocarriers with encapsulated magnetic nanoparticles for controlled drug release†

Shun Yang, Dongyun Chen, Najun Li,* Xiao Mei, Xiuxiu Qi, Hua Li, Qingfeng Xu and Jianmei Lu*

Received 21st July 2012, Accepted 10th October 2012

DOI: 10.1039/c2jm34817a

Novel multifunctional nanocomposites were successfully prepared for the controlled release of anti-cancer drug and magnetic resonance imaging (MRI) *via* a simple self-assembly process. In this strategy, superparamagnetic iron oxide nanoparticles (SPIONPs) were “fixed” between the hydrophobic segment of the pH-sensitive amphiphilic polymer (HAMAFA-*b*-DBAM) and the surface of hollow mesoporous silica nanoparticles (HMS) which were modified by the long-chain hydrocarbon octadecyltrimethoxysilane (C18). Since the amphiphilic polymer was conjugated with a folic acid (FA) group, the nanocomposites could target the folic acid receptor (FR) of over-expressed tumor cells efficiently. Moreover, high drug loading content was obtained simultaneously due to the hollow core of HMS. The loaded drug could release from the HMS core triggered by the mildly acidic pH environment in the cancer cells due to the hydrolysis of the pH-sensitive polymer shell. The targeting process of the nanocomposites could be easily tracked by MRI due to the magnetism of the SPIONPs. Therefore, a nanocarrier with high drug-loading capacity and controlled drug release property for tumor diagnosis and therapy was obtained *via* the self-assembly of HMS core, magnetic Fe₃O₄ nanoparticles and targetable pH-sensitive polymer shell.

Introduction

Inorganic nanoparticles such as gold nanoparticles,¹ mesoporous silica nanoparticles,^{2,3} Fe₃O₄ nanoparticles⁴ have been increasingly used to prepare nanocomposites for biomedical applications. Among them, superparamagnetic iron oxide nanoparticles (SPIONPs) and hollow mesoporous silica nanoparticles (HMS) have attracted great attention in the past few years. As a magnetic resonance imaging (MRI) contrast agent, SPIONPs have been widely used for cell imaging due to their superparamagnetism, narrow size distributions and imaging sensitivity.^{5,6} HMS are also currently used in the field of drug delivery due to their unique biocompatibility and chemical stability. Notably, the hollow core and silica shell endow the HMS with a high drug loading capacity and a modifiable outer surface.^{7–10}

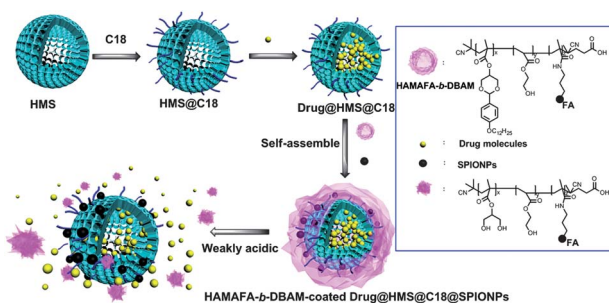
In view of the above, many researchers fabricated various nanocomposites containing both Fe₃O₄ and silica. For instance, Gai and co-workers reported a facile method in which the hydrophobic SPIONPs were absorbed on the cetyltrimethylammonium bromide (CTAB) template, and then silicate molecules were assembled on the surface to form a silica shell for further modification.^{11,12} However, these inorganic

nanocomposites are able to achieve controlled release when acting as drug carriers despite their complicated preparation process. Recently, stimuli-responsive (*e.g.* pH changes, temperature, enzyme, redox or light) block copolymer micelles are particularly attractive for controlled drug release.^{13–21} The promising method is the modification of inorganic nanoparticles with stimuli-responsive copolymers to achieve controlled release for drug delivery applications.^{22,23} In our previous works, pH-responsive amphiphilic polymers were employed to encapsulate HMS for targeted anti-cancer drug release. High drug loading capacity was obtained in this approach and they could release incorporated drugs selectively in mildly acidic tumor sites.²⁴ Thus, we envisioned that if we introduce the hydrophobic SPIONPs into this self-assembly process, the pH-responsive amphiphilic polymers would encapsulate SPIONPs and HMS together and the obtained nanocomposites could act as both a contrast agent for MRI and highly efficient nanocarriers for cancer therapy.

Herein, we report a facile strategy to prepare a multifunctional nanocomposite for controlled anti-cancer drug delivery and MRI imaging *via* a simple self-assembly process. SPIONPs stabilized by oleic acid are “fixed” between the hydrophobic part of the polymer and the surface of HMS which were modified with the long-chain hydrocarbon octadecyltrimethoxysilane (C18) (Scheme 1). The resulting nanocomposites have several advantages as follows. First, a high drug loading content could be achieved due to the hollow core of the HMS; the long alkyl chains grown on the shell are able to delay the drug release. Second, the drug delivery process could be easily tracked by MRI

Key Laboratory of Organic Synthesis of Jiangsu Province, College of Chemistry, Chemical Engineering and Materials Science, Soochow University, Suzhou, China, 215123. E-mail: lujm@suda.edu.cn; linajun@suda.edu.cn; Fax: +86 (0) 512-6588 0367; Tel: +86 (0) 512-6588 0368

† Electronic supplementary information (ESI) available. See DOI: 10.1039/c2jm34817a



Scheme 1 Schematic depiction of the structure of HAMAFA-*b*-DBAM-coated DOX@HMS@C18@SPIONPs and controlled release by degradation under weakly acidic conditions.

due to the SPIONPs encapsulated in the nanocomposites. Moreover, compared to other amphiphilic polymers, our pH-responsive polymer conjugated with folic acid (FA) moiety is more suitable for targeted anti-cancer drug delivery. When recognized by the FA receptor of positive tumor cells, the nanocarriers could be internalized efficiently with subsequent controlled release of the loaded drug. Most importantly, in this facile strategy, an amphiphilic polymer was introduced to encapsulate hydrophobic SPIONPs and HMS in one nanosystem and this could also be used to combine another kinds of small size inorganic nanoparticles with HMS to form multifunctional nanocomposites for further applications.

Experimental section

Materials

(2-(Acryloyloxy)ethyl)trimethylammonium chloride (AETAC, 80 wt% in water), 2,2'-azobis(2-methylpropionamide) dihydrochloride (V-50, >97.0%), hexadecyltrimethylammonium bromide (CTAB, >99.0%) and octadecyltrimethoxysilane (C18) were purchased from Aldrich. Tetraethoxysilane (TEOS) was purchased from Alfa without any further purification. Styrene (St, >99.0%) was washed through an inhibitor remover column for removal of *tert*-butyl catechol and then distilled under reduced pressure prior to use. Ferric trichloride hexahydrate ($\text{FeCl}_3 \cdot 6\text{H}_2\text{O}$), sodium oleate, sodium methoxide, potassium ferricyanide, *p*-hydroxybenzaldehyde, benzyl chloride, 1-bromododecane, *p*-toluene sulfonic acid (PTSA) and glycerol were all purchased from Shanghai Chemical Reagent Co. Ltd as analytical reagents and used without further purification. 4,4'-Azobis(4-cyanovaleric acid) (V-501) and azobisisobutyronitrile (AIBN) were purchased from Aldrich. *N*-Hydroxysuccinimide (NHS, 99%), *N*-(3-aminopropyl)methacrylamide hydrochloride (APMA), dicyclohexcarbodiimide (DCC, 99%) and 4-dimethylaminopyridine (DMAP, 99%) were purchased from Alfa Aesar. Methacryloyl chloride was produced from Haimen Best Fine Chemical Industry Co. Ltd and used after distillation. Hydroxyethylacrylate (HEA) was distilled under vacuum and stored at 15 °C under an inert gas atmosphere. Other reagents were commercially available and used as received.

Synthesis of hollow mesoporous spherical (HMS) particles

The hollow mesoporous spherical particles were synthesized according to the literature with little modification.²⁵ To prepare

the PS latex templates, 0.5 g AETAC (80 wt% in H_2O) was dissolved in 180 g water in a 500 ml round-bottom flask. Then 20.0 g styrene was added slowly and kept stirring for 30 min. The mixture was purged with nitrogen for 20 min and then heated to 90 °C. Afterwards, 5 ml of an aqueous solution containing 0.5 g V-50 was added. The emulsion was kept at 90 °C for 24 h under nitrogen to complete the polymerization. The polystyrene latex was collected by centrifugation and washed with ethanol several times. To prepare the HMS, 0.8 g CTAB was dissolved in a mixture of 80.0 g water, 60.0 g ethanol and 1.5 ml ammonium hydroxide solution. 0.93 g of PS powders was dispersed in 10.0 g water by sonication and then added dropwise to the above CTAB solution at room temperature with vigorous stirring, followed by sonication for 10 min. The derived milky mixture was then stirred for 30 min before adding 4.0 g TEOS. The mixture was kept stirring at room temperature for 48 h. The precipitate was collected by centrifugation and washed with ethanol, then dried at room temperature. Finally the material was calcined in air at 600 °C for 8 h to remove any organic matter.

Modification of the external surface of HMS with octadecyltrimethoxysilane (C18)

100 mg HMS was first dispersed in 20 ml anhydrous acetonitrile, then 5 ml C18 was added, and the obtained suspension was stirred for 24 h and collected by centrifugation, washed with acetonitrile and ethanol several times, and dried under vacuum.

Preparation of superparamagnetic iron oxide nanoparticles (SPIONPs)

SPIONPs were synthesized according to the literature with some modifications.²⁶ 2.7 g (10 mmol) $\text{FeCl}_3 \cdot 6\text{H}_2\text{O}$ and 9.1 g (30 mmol) sodium oleate were dissolved in a mixed solvent composed of 20 ml ethanol, 15 ml water and 35 ml hexane. After heating at 70 °C for 4 h, the organic layer was washed and evaporated to obtain an iron-oleate complex. Then 9.0 g (10 mmol) of the iron-oleate complex and 1.4 g oleic acid (5 mmol) were dissolved in 50 g trioctylamine at room temperature. The obtained nanoparticles were washed several times with ethanol and dried at 60 °C for 24 h.

Synthesis of RAFT agent 4-cyanopentanoic acid dithiobenzoate (CAD)

CAD was synthesized according to the literature with some modifications.²⁷ Briefly, 12.8 g benzyl chloride was added dropwise to a sodium methoxide methanol solution (172 g, 12.6 wt%) containing 12.8 g elemental sulfur. Subsequently, the obtained mixture was refluxed for 10 h under an inert atmosphere. The crude sodium dithiobenzoate solution was extracted by diethyl ether, 1.0 M hydrochloric acid and sodium hydroxide aqueous solution and finally yielded a solution of sodium dithiobenzoate. Potassium ferricyanide solution (500 ml, 6.5 wt%) was added dropwise to the sodium dithiobenzoate over a period of 1 h with vigorous stirring. The obtained red precipitate was filtered, washed with deionized water, and dried under vacuum at room temperature overnight. Dithiobenzoyl disulfide (8.50 g, 0.28 mol) was added slowly to the distilled ethyl acetate (150.0 ml) solution containing 11.68 g V-501 (0.42 mol). After refluxing for 18 h, the

reaction solution was concentrated under vacuum and purified by column chromatography (ethyl acetate–hexane, 2 : 3). ^1H NMR (400 MHz, CDCl_3), δ (ppm): 7.91 (d, $J = 7.59$ Hz, 2H, C_6H_4), 7.58 (t, $J = 7.47$ Hz, 1H, C_6H_4), 7.41 (t, $J = 7.79$ Hz, 2H, C_6H_4), 2.75 (m, 2H, CCH_2), 2.45 (m, 2H, CH_2COOH), 1.95 (s, 3H, CH_3).

Synthesis of 4-*n*-dodecyloxybenzalacetal monomer (DBAM)

4-*n*-Dodecyloxybenzaldehyde (DBD) was synthesized according to the literature with some modification.²⁸ 1-Bromododecane (29.9 g, 120 mmol) was added dropwise to the mixture of *p*-hydroxybenzaldehyde (12.2 g, 10 mmol) and anhydrous potassium carbonate (20.7 g, 150 mmol) in 150 ml acetone. After heating under reflux with stirring for 14 h, the mixture was filtered off and acetone was removed by a rotary evaporator. The crude product was purified by column chromatography with a mixture of ethyl acetate–petroleum ether (boiling range 60–90 °C) (1/10, v/v). ^1H NMR (400 MHz, CDCl_3), δ (ppm): 9.88 (s, 1H, CHO), 7.83 (d, $J = 8.72$ Hz, 2H, C_6H_4), 6.99 (d, $J = 8.69$ Hz, 2H, C_6H_4), 4.04 (t, $J = 6.56$ Hz, 2H, CH_2O), 1.86–1.76 (m, 2H, $\text{CH}_2\text{CH}_2\text{O}$), 1.46 (m, 2H, $\text{CH}_2\text{CH}_2\text{CH}_2\text{O}$), 1.26 (m, 16H, CH_2), 0.88 (t, $J = 6.79$ Hz, 3H, CH_3).

After that, DBD (8.7 g, 30 mmol) was reacted with glycerol (2.76 g, 30 mmol) in 50 ml toluene using PTSA (0.5 g) as the catalyst. The solution was refluxed for 14 h and the water formed by dehydrogenation reaction was removed by the oil–water separator. Then, the mixture was concentrated and washed with potassium carbonate solution (1%, 80 ml) to remove the acid catalyst and any residual glycerol. After that, the precipitate was collected and purified by column chromatography with a mixture of ethyl acetate–petroleum ether (1/2, v/v) to obtain 4-*n*-dodecyloxybenzalacetal (DBA). ^1H NMR (400 MHz, CDCl_3), δ (ppm): 7.41 (d, $J = 8.51$ Hz, 2H, C_6H_4), 6.90 (d, $J = 8.67$ Hz, 2H, C_6H_4), 5.51 (s, 1H, $\text{C}_6\text{H}_4\text{CH}$), 3.57–4.38 (m, 8H, $\text{C}_6\text{H}_4\text{OCH}_2$, CHCH_2O , CHOH , OH), 1.86–1.76 (m, 2H, $\text{CH}_2\text{CH}_2\text{O}$), 1.50–1.39 (m, 2H, $\text{CH}_2\text{CH}_2\text{CH}_2\text{O}$), 1.26 (m, 16H, CH_2), 0.88 (t, $J = 6.78$ Hz, 3H, CH_3).

Methacryloyl chloride (2.3 g, 22 mmol) was added slowly to the anhydrous tetrahydrofuran (20 ml) solution containing triethylamine (4.5 g, 44 mmol) and DBA (4.0 g, 11 mmol) and cooled to 0 °C in a water–ice bath. After constantly stirring for another 12 h at room temperature, the mixture was filtered off to remove the byproduct. The obtained filtrate was concentrated and purified by column chromatography with a mixture of ethyl acetate–petroleum ether (1/8, v/v). ^1H NMR (400 MHz, CDCl_3), δ (ppm): 7.41 (d, $J = 8.39$ Hz, 2H, C_6H_4), 6.89 (d, $J = 8.41$ Hz, 2H, C_6H_4), 6.30 (s, 1H, CCH_2), 5.65 (s, 1H, CCH_2), 5.52 (s, 1H, $\text{C}_6\text{H}_4\text{CH}$), 4.75 (s, 1H, CHO), 4.31 (d, $J = 12.88$ Hz, 2H, CHCH_2O), 4.18 (d, $J = 12.92$ Hz, 2H, CHCH_2O), 3.95 (t, $J = 6.59$ Hz, 2H, $\text{C}_6\text{H}_4\text{OCH}_2$), 2.01 (s, 3H, CH_3), 1.81–1.72 (m, 2H, $\text{CH}_2\text{CH}_2\text{O}$), 1.49–1.38 (m, 2H, $\text{CH}_2\text{CH}_2\text{CH}_2\text{O}$), 1.26 (m, 16H, CH_2), 0.88 (t, $J = 6.68$ Hz, 3H, CH_2CH_3).

Synthesis of HAMA-*b*-DBAM

HAMA was prepared by RAFT polymerization of HEA and APMA using CAD as a transfer agent according to the literature with some modification.²³ Typically, 5.3 mg (0.02 mmol) CAD

was added to the aqueous solution containing 2.5 mg V-501, 1.22 g HEA (10.5 mmol) and 268 mg APMA (1.5 mmol). Then the tube was sealed after three cycles between vacuum and nitrogen. After 5 h reaction in an oil bath at 70 °C, the mixture was concentrated and washed with a large amount of acetone. The obtained copolymer was dried under vacuum and stored in desiccators for further polymerization.

The amphiphilic diblock polymer HAMA-*b*-DBAM was synthesized using HAMA macro chain transfer agent. In a typical polymerization procedure, 1.2 g HAMA was added to a dimethylsulfoxide solution containing 3 mg AIBN and 200 mg (0.31 mmol) DBAM and then placed in an oil bath at 70 °C for 5 h. The mixture was concentrated and washed with a large amount of ethyl ether. After washing, the obtained diblock polymer was dried under vacuum overnight and stored in desiccators.

Synthesis of folate conjugated diblock polymer HAMAFA-*b*-DBAM

The conjugation procedure was carried out according to the literature reported elsewhere.^{29–31} First, the thiocarbonylthio end group of HAMA-*b*-DBAM was removed according to the literature with some modifications. Briefly, 500 mg HAMA-*b*-DBAM was dissolved in 10 ml *N,N*-dimethylformamide (DMF) containing 30 mg AIBN. The DMF solution was sealed after cycling between vacuum and nitrogen three times. After stirring at 70 °C for 5 h, the mixture was precipitated in anhydrous ether. The obtained diblock polymer was dried under vacuum and stored in desiccators for further use. Second, folate NHS ester was prepared by the following procedure: 0.62 g DCC and 0.51 g NHS were added to a dry dimethylformamide (50 ml) solution containing 2.0 g folic acid and then the solution was stirred for 12 h at room temperature in the dark. The solution was filtered off and precipitated in diethyl ether. The obtained yellow powder was washed several times with anhydrous ether and used immediately for the next step. Then, FA-NHS (30 mg) was added to dry pyridine containing 100 mg of the above polymer. The solution was shaken for 12 h at room temperature and the mixture was precipitated in 40% acetone in diethyl ether. The filtrate was concentrated and stored in the dark at 4 °C. ^1H NMR (400 MHz, $\text{DMSO}-d_6$), δ (ppm): 8.63–6.62 (folic acid and CH_2NH_2), 4.21–3.76 ($\text{COOCH}_2\text{CH}_2$ and CH_2OH), 2.85 (NHCH_2 and CH_2NH_2), 1.21 (CH_3).

Synthesis of HAMAFA-*b*-DBAM-coated HMS@C18@SPIONPs

Oleic acid-stabilized SIONPs (5 mg) and HMS (10 mg) were dispersed in 750 μl tetrahydrofuran by sonication for 5 min to get solution A, then HAMAFA-*b*-DBAM (20 mg) was dissolved in tetrahydrofuran (750 μl) to get solution B. Solution B was combined with solution A in an ultrasonic bath at room temperature for 5 min. Then, 5 ml distilled water was added to the above solution with vigorous shaking and the resulting colloid was stirred vigorously for 24 h to evaporate the tetrahydrofuran.

In vitro experiments

In vitro drug-release. To evaluate the drug loading capacity and release properties, doxorubicin (DOX) was used as the model drug according to the literature with some modifications.^{9,32} DOX was extracted from doxorubicin hydrochloride (DOX·HCl) according to the procedure reported previously.³³ HMS@C18 (4, 2 and 0.4 mg ml⁻¹) were dispersed into 1 ml SBF buffer solution, then DOX solution (5 mg ml⁻¹, 40 µL) was added. After dispersion and stirring under light-sealed conditions for 24 h, DOX@HMS@C18 were obtained by centrifugation and washed with 20 ml of PBS (pH 7.4), then dried at 60 °C in vacuum. HAMAFA-*b*-DBAM-coated DOX@HMS@C18@SPIONPs was prepared *via* self-assembly as discussed before. Then, 5 mg of sample was immersed in simulated body fluid (SBF) incubated at 37 °C to maintain a constant temperature. The obtained colloid was divided into two equivalent parts and adjusted to different pH values by acetate buffer.

Here, the DOX concentration was determined using a fluorescence spectrophotometer at $\lambda_{\text{ex}} = 480$ nm and $\lambda_{\text{em}} = 627$ nm. A standard plot was prepared under identical conditions to confirm the amount of drug loaded by HMS@C18. Drug loading content and drug loading efficiency can be calculated as follows:

Drug loading content (wt%) = (weight of loaded drug/weight of nanocomposites) \times 100%;

Drug loading efficiency (%) = (weight of loaded drug/weight of drug in feed) \times 100%.

Cell culture and preparation. A549 human alveolar adenocarcinoma (FR-) and human KB (FR+) cell lines (purchased from Shanghai Cell Institute Country Cell Bank, China) were cultured as monolayers in RPMI-1640 medium supplemented with 10% heat-inactivated fetal bovine serum at 37 °C in a humidified incubator (5% CO₂ in air, v/v).

In vitro cytotoxicity. The aminoxanthene dye, sulforhodamine B (SRB), was used as an assay for assessing the effects of drug carriers in various concentrations.³⁴ In brief, well-growing KB cells were placed in 96-well plates (1.3 \times 10⁴ cells per well) and four duplicate wells were set up in the sample. The culture medium was replaced with a medium containing different concentrations of drug carriers and cultured at 37 °C in a humidified incubator (5% CO₂ in air, v/v) with the cells anchored to the plates. After being cultured for 24 h, the medium was poured away and 10% (w/v) trichloroacetic acid in Hank's balanced salt solution (100 ml) was added and stored at 4 °C for 1 h. Then the stationary liquid was discarded, the cells were washed with deionized water five times before air drying and stained with 0.4% (w/v) SRB solution (100 ml per well) for 30 min at room temperature. After removing the SRB, the cells were washed with 0.1% acetic acid solution five times. Bound SRB dye was solubilized with 10 mmol l⁻¹ Tris-base solution (150 ml, pH = 10.5). The optical density (OD) value of each individual well was calculated using a spectrophotometer at 531 nm absorbance.

Cellular uptake of HAMAFA-*b*-DBAM-coated DOX@HMS@C18@SPIONPs. Herein, doxorubicin (DOX)

was used as model anticancer agent owing to its fluorescence that is convenient to be observed by confocal laser fluorescence microscopy. KB cells were seeded in 96-well plates (1.3 \times 10⁴ cells per well) and incubated overnight at 37 °C in a humidified incubator. The sample of HAMAFA-*b*-DBAM-coated DOX@HMS@C18@SPIONPs was dispersed in RPMI-1640 medium. Cells were cultured with the HAMAFA-*b*-DBAM-coated DOX@HMS@C18@SPIONPs solution for a certain time and observed using confocal laser fluorescence microscopy (Olympus, FV 1000) after washing three times with PBS.

MRI experiments

MRI experiments were carried out with a 0.5 tesla (T) superconducting unit (GE Vectra, International General Electric, Slough, UK). HAMAFA-*b*-DBAM-coated HMS@C18@SPIONPs was loaded into Eppendorf tubes for imaging. Multi-section *T*₂-weighted fast spin-echo sequences were performed in at least two orthogonal planes to obtain MR phantom images. MRI signal intensity was calculated using the in-built software.

Characterization

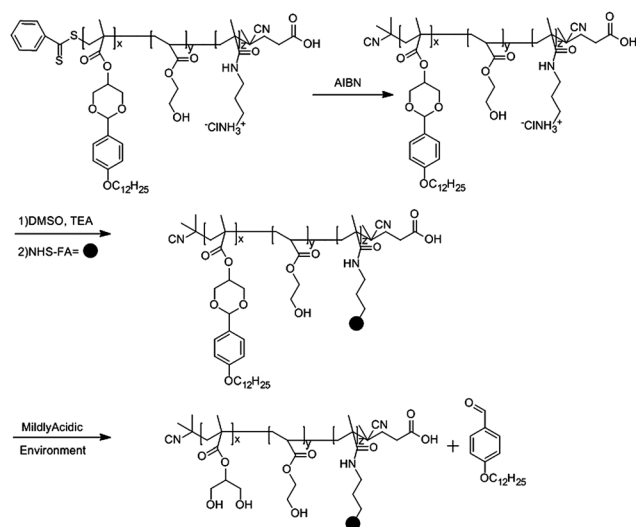
FT-IR measurements were performed as KBr pellets on a Nicolet 4700 spectrometer (Thermo Fisher Scientific) in the range of 400–4000 cm⁻¹. ¹H NMR spectra were measured by an INOVA 400 MHz NMR instrument. TEM images were obtained using a TecnaiG220 electron microscope at an acceleration voltage of 200 kV. Energy dispersive spectrometry (EDS) was taken on a Hitachi S-4700 equipped with an energy-dispersive X-ray spectrometer. Brunauer–Emmett–Teller (BET) and Barrett–Joyner–Halenda (BJH) analyses were used to determine the surface area, pore size and pore volume and measurements were obtained with a Quantachrome Autosorb 1C apparatus at -196 °C under continuous adsorption conditions. Confocal laser scanning microscopy (CLSM) images were observed by a confocal laser scanning microscope (Olympus, FV 1000).

Results and discussion

Synthesis of HAMAFA-*b*-DBAM and DOX@HMS@C18

The amphiphilic copolymer used here was synthesized as in a previous report,²³ which is shown in Scheme 2. The ¹H NMR spectrum of HAMAFA-*b*-DBAM (not listed here, but the characteristic data are listed above in the experimental section) showed the successful conjugation of FA. When specifically recognized and internalized by tumor cells, the pH-responsive polymer would hydrolyze into a biocompatible polymer due to cleavage of acetal moieties in the weakly acidic endosomal/lysosomal compartments, the hydrophobic segments hydrolyzed into hydrophilic segments, resulting in encapsulated drug release from unblocked pores of HMS.

The surface of HMS has many Si-OH groups,^{2,3,35} which could be simply modified with C18. As can be seen, there was no change in the diameter of particles between HMS and HMS@C18. N₂ adsorption-desorption isotherms and the corresponding pore size distributions of HMS, HMS@C18 are shown in Fig. S1.†



Scheme 2 Schematic illustration of the synthesis of HAMAFA-*b*-DBAM.

The FT-IR spectra of HMS, HMS@C18 and DOX@HMS@C18 are shown in Fig. 1. The Si–OH bond (950 cm^{-1}) in the spectrum of HMS suggested that a large number of silanol groups exist on the surface of HMS for coupling alkyl chains. As shown in the spectrum of HMS@C18, a strong bond of C–H_x (2890 cm^{-1}) revealed the successful growth of alkyl chains on the silica. For the DOX@HMS@C18, a new bond of C=O (1740 cm^{-1}) appeared according to the spectrum of HMS@C18, implying that the DOX molecules were loaded into the nanoparticles successfully.

Assembly of HAMAFA-*b*-DBAM-coated HMS@C18@SPIONPs

The surface of the HMS shell was first modified with C18 to change the wettability of the particle, and TEM images of HMS (Fig. 2a) and HMS@C18 (Fig. 2b) did not show any difference. Then, the nanocomposite was prepared through a self-assembly process. First, SPIONPs and HMS@C18 were dispersed in tetrahydrofuran by sonication to get solution A, the oleic acid-capped SPIONPs could be absorbed on the surface of HMS@C18 *via* hydrophobic interactions. HAMAFA-*b*-DBAM

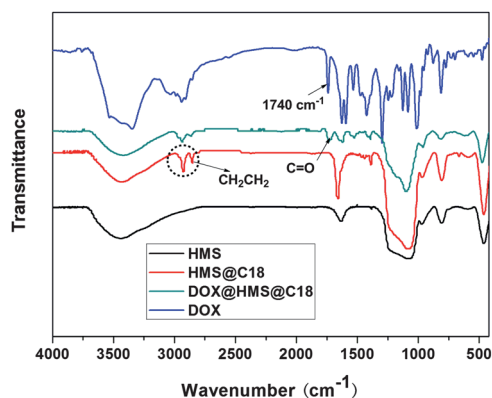


Fig. 1 FT-IR spectra of HMS, HMS@C18 and DOX@HMS@C18.

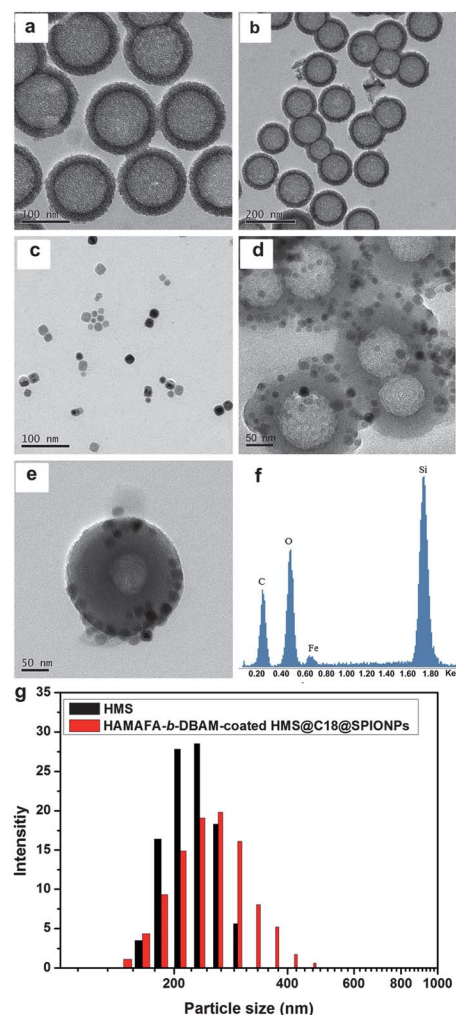


Fig. 2 TEM images of HMS (a), HMS@C18 (b), oleic acid-capped SPIONPs (c), HAMAFA-*b*-DBAM-coated HMS@C18@SPIONPs (d and e), EDS spectrum of HAMAFA-*b*-DBAM-coated HMS@C18@SPIONPs (f) and DLS of HMS and HAMAFA-*b*-DBAM-coated HMS@C18@SPIONPs (g).

was dissolved in tetrahydrofuran (solution B) and the solution was immersed into solution A slowly. Then, 5 ml of distilled water was added to the above solution, and THF was evaporated under continued shaking, the amphiphilic polymer would form micelles to encapsulate the hydrophobic guest molecules. The obtained HAMAFA-*b*-DBAM-coated HMS@C18@SPIONPs remained hydrophilic because of the hydrophilic segment of HAMAFA-*b*-DBAM. The detailed morphological and structural features of the prepared nanoparticles were examined by TEM. Comparing with HMS@C18 and SPIONPs (Fig. 2c), we can clearly see that SPIONPs stabilized by oleic acid were fixed between the hydrophobic part of the polymer and the outer surface of HMS@C18. The prepared HAMAFA-*b*-DBAM-coated HMS@C18@SPIONPs (Fig. 2d and e) have an average diameter of about 200 nm and maintained good monodispersity and the DLS shows nearly the same result (Fig. 2g). The EDS spectrum (Fig. 2f) of HAMAFA-*b*-DBAM-coated HMS@C18@SPIONPs was used to further confirm the presence of silicon (HMS) and iron (SPIONPs) (10%). Thus, the

nanoparticles formed by HMS, SPIONPs and HAMAFA-*b*-DBAM were successfully synthesized.

Drug loading and release

To discuss the drug loading and release behaviours of the HAMAFA-*b*-DBAM-coated HMS@C18@SPIONPs, DOX was used as the model anticancer agent. The drug loading content was determined by measuring drug concentrations before and after being loaded by HMS@C18. The theoretical drug loading contents were set at 5%, 10% and 50%. DOX loading efficiency was measured at 82, 81 and 77% (Table 1). Then HAMAFA-*b*-DBAM-coated DOX@HMS@C18@SPIONPs were prepared through a self-assembly process at a low drug loading content (*ca.* 5 wt%),³⁶ and by evaluating the DOX concentration after the centrifugation of nanocomposites, 5.6% of the DOX loaded in the HMS was lost in this process. However, the drug loading content presented that HMS was much more suitable for drug delivery than common mesoporous silica owing to its hollow core. Furthermore, the hydrophobic surface of HMS modified by long alkyl chains made the insoluble drug molecules more easily loaded.

Herein, we used SBF with different pH values (pH = 5.0 and 7.4) at 37 °C to simulate the tumor and normal cells and the *in vitro* drug release behaviour of HAMAFA-*b*-DBAM-coated DOX@HMS@C18@SPIONPs is shown in Fig. 3. About 70% of DOX was released from the HMS at pH 5.0 while only less than 5% of DOX was released in a neutral environment after 150 h. This phenomenon strongly demonstrated that the polymer could degrade in an acidic environment due to its pH-sensitive groups and then turned hydrophilic to allow drug release from the unblocked pores of HMS.³⁷ However, the SPIONPs attached to silica did not affect the DOX release a lot. Hence, the highly pH-sensitive polymer used here was able to prevent the drug release in a normal physiological environment, which was desirable for selective drug release. Besides, the long alkyl chains could delay the drug release to about 150 h due to the hydrophobic interaction between drug and long alkyl chains, so that a long-term drug release was obtained, which is important for further cancer treatment.

Evaluation of cytotoxicity and drug uptake

The sulforhodamine B (SRB) assay was used to assess the cytotoxicity of the nanocomposite. After incubation in the nanocomposite for 72 h, the cells displayed high cell viability (>80%) as shown in Fig. 4. Even at a high concentration, the cytotoxicity still remained at a low level. The result above proved the polymer shell to be biocompatible and nontoxic.

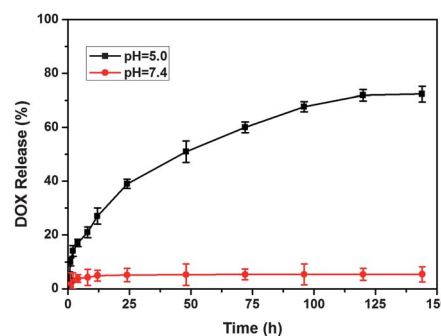


Fig. 3 Release of DOX *in vitro* from drug-loaded HAMAFA-*b*-DBAM-coated DOX@HMS@C18@SPIONPs at different pH at 37 °C.

These characteristics are necessary for further biomedical application.

Since DOX is a fluorophore, the fluorescence intensity could be used to evaluate the intracellular activity of the obtained nanocomposites in folate receptor positive (KB cells) and negative (A549) cancer cell lines. Herein, *in vitro* experiments based on these two cells were used to demonstrate the selective release and targeting properties of the nanocomposites. KB and A549 cells' uptake and the intracellular distribution of the nanocomposites with FA groups were studied by CLSM. And after being incubated with nanocomposites for 0.5 h and 2 h, the DOX distributions are shown in Fig. 5.

To quantify the cellular uptake of nanocarriers for the two different cell lines, the mean fluorescence intensity of FR+ and FR- cells with HAMAFA-*b*-DBAM-coated DOX@HMS@C18@SPIONPs in solution at different incubation times are shown in Fig. S2.† No significant difference could be observed in the fluorescence intensity between the two nanocomposites when

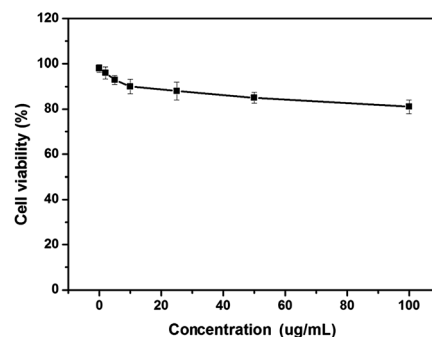


Fig. 4 *In vitro* cell viability of DOX-free HAMAFA-*b*-DBAM-coated HMS@C18@SPIONPs at different concentrations.

Table 1 Drug loading content and drug loading efficiency

Theoretical drug loading content (wt%)	Drug loading content ^a (wt%)	Drug loading efficiency (%)
5	4.1	82
10	8.1	81
50	38.5	77

^a Drug loading content for DOX was determined by fluorescence measurements.

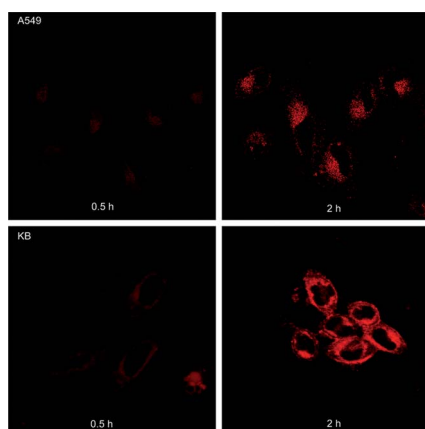


Fig. 5 CLSM of FR[−] and FR⁺ incubated with HAMAFA-*b*-DBAM-coated DOX@HMS@C18@SPIONPs for 0.5 h and 2 h.

incubated for 0.5 h. But after 2 h, a significant increase in fluorescence intensity can be seen in KB cells incubated with FA-conjugated nanocomposites. This result demonstrated that in a short time the nanocomposites were internalized by the KB and A549 cells through a same endocytosis process. 2 h later, the changes in fluorescence intensity demonstrated that the targeting moiety offered by folic acid is efficient at enhancing the tumor cell targeting *in vitro* because the FA-conjugated nanocomposite was taken up by KB cells through a folate receptor-mediated endocytosis.^{38–41}

Magnetic properties

The as-fabricated nanocomposites have a strong magnetism due to the Fe₃O₄ nanoparticles capped by the polymer. HAMAFA-*b*-DBAM-coated HMS@C18@SPIONPs had homogeneous dispersions in water and a serum-containing medium (Fig. S3†), and showed a sensitive response to an external magnetic field: a visible separation could be seen just about 5 min later (Fig. 6c). Furthermore, to evaluate the detectability of the nanocomposite, the magnetic resonance phantom imaging method was used. The *T*₂-weighted phantom images of the nanocomposites at different concentrations are shown in Fig. 6a. Even at a low concentration, the prepared nanocarriers still have a strong signal intensity.⁴² Fig. 6b shows the relaxation rate. The specific relaxivity is

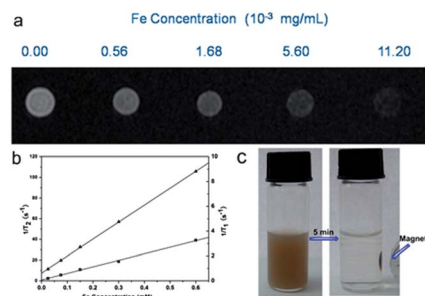


Fig. 6 (a) *T*₂-weighted MR images, (b) relaxation rates (*1/T*₁ and *1/T*₂) of HAMAFA-*b*-DBAM-coated SPIONPs@HMS@C18 at various Fe concentrations and (c) photograph of the separation process of HAMAFA-*b*-DBAM-coated SPIONPs@HMS@C18.

5.2 and 165 mM^{−1} s^{−1} for *r*₁ and *r*₂, respectively. In our study, the relaxivity of *r*₁/*r*₂ is calculated to be 32, which is much larger than that of commercial dextran-coated SPIONPs.⁴³ To study the intracellular accumulation of SPIONPs, KB cells were incubated with nanocomposites for 0.5 h, and the Prussian Blue-staining results are shown in Fig. S4.† Good magnetic responsivity and effective imaging ability of HAMAFA-*b*-DBAM-coated HMS@C18@SPIONPs revealed their potential applications for targeting and separation as a drug carrier.

Conclusion

In summary, we have designed a multifunctional nanocomposite for anti-cancer drug delivery *via* a simple self-assembly strategy. In this strategy, the oleic acid-capped SPIONPs were used without any modifications, the HMS were modified with long alkyl chains and turned hydrophobic. And then a FA-conjugated pH-sensitive amphiphilic polymer was introduced to cap the two inorganic nanoparticles *via* a simple self-assembly process. The as-prepared nanocomposite could not only act as an efficiency drug carrier due to its high drug loading content, pH-dependent degradation and cancer targeting group, but could also be used to track the cancer targeting process due to its magnetism. Most importantly, this reported facile strategy could be used to combine other inorganic nanoparticles with silicon for further applications.

Acknowledgements

We acknowledge that funding for this work came from National Natural Science Foundation of China (20902065, 21076134), Supporting Project for Science and Technology of Jiangsu Province (Industry) (BE2011074), Natural Science Foundation of Jiangsu Province (BK2012625), a Project Funded by the Priority Academic Program Development of Jiangsu Higher Education Institutions (PAPD) and Innovative Research Team of Advanced Chemical and Biological Materials, Suzhou University.

Notes and references

- M. C. Daniel and D. Astruc, *Chem. Rev.*, 2004, **104**, 293.
- J. Lu, M. Liong, Z. X. Li, J. I. Zink and F. Tamanoi, *Small*, 2010, **6**, 1794.
- H. Meng, M. Xue, T. Xia, Y. L. Zhao, F. Tamanoi, J. F. Stoddart, J. I. Zink and A. E. Nel, *J. Am. Chem. Soc.*, 2010, **132**, 12690.
- J. Xie, C. Xu, N. Kohler, Y. Hou and S. Sun, *Adv. Mater.*, 2007, **19**, 3163.
- R. Hao, R. Xing, Z. Xu, Y. Hou, S. Gao and S. Sun, *Adv. Mater.*, 2010, **22**, 2729.
- H. Lee, E. Lee, N. K. Jang, Y. Y. Jeong and S. Jon, *J. Am. Chem. Soc.*, 2006, **128**, 7383.
- W. R. Zhao, M. D. Lang, Y. S. Li, L. Li and J. L. Shi, *J. Mater. Chem.*, 2009, **19**, 2778.
- Y. Chen, H. R. Chen, L. M. Guo, Q. J. He, F. Chen, J. Zhou, J. W. Feng and J. L. Shi, *ACS Nano*, 2010, **4**, 529.
- Y. F. Zhu, J. L. Shi, W. H. Shen, X. P. Dong, J. W. Feng, M. L. Ruan and Y. S. Li, *Angew. Chem., Int. Ed.*, 2005, **44**, 5083.
- X. Mei, S. Yang, D. Y. Chen, N. J. Li, H. Li, Q. F. Xu, J. F. Ge and J. M. Lu, *Chem. Commun.*, 2012, **48**, 10010.
- S. L. Gai, P. P. Yang, P. A. Ma, D. Wang, C. X. Li, N. Xiu and J. Lin, *J. Mater. Chem.*, 2011, **21**, 16420–16426.
- C. Ren, J. Li, X. Chen, Z. Hu and D. Xue, *Nanotechnology*, 2007, **18**, 345604.

- 13 R. M. Sawant, J. P. Hurley, S. Salmasso, A. Kale, E. Tolcheva, T. S. Levchenko and V. P. Torchilin, *Bioconjugate Chem.*, 2006, **17**, 943.
- 14 D. Schmaljohann, *Adv. Drug Delivery Rev.*, 2006, **58**, 1655.
- 15 A. K. Bajpai, S. K. Shukla, S. Bhanu and S. Kankane, *Prog. Polym. Sci.*, 2008, **33**, 1088.
- 16 S. Ganta, H. Devalapally, A. Shahiwala and M. Amiji, *J. Controlled Release*, 2008, **126**, 187.
- 17 L. Linderroth, G. H. Peters, R. Madsen and T. L. Andresen, *Angew. Chem.*, 2009, **121**, 1855.
- 18 H. Koo, H. Lee, S. Lee, K. H. Min, M. S. Kim, D. S. Lee, Y. Choi, I. C. Kwon, K. Kim and S. Y. Jeong, *Chem. Commun.*, 2010, **46**, 5668.
- 19 J. Y. Ko, S. Park, H. Lee, H. Koo, M. S. Kim, K. Choi, I. C. Kwon, S. Y. Jeong, K. Kim and D. S. Lee, *Small*, 2010, **6**, 2539.
- 20 Y. Zhao, *Macromolecules*, 2012, **45**, 3647.
- 21 J.-M. Schumers, C.-A. Fustin and J.-F. Gohy, *Macromol. Rapid Commun.*, 2010, **31**, 1588.
- 22 K. Miyata, M. Oba, M. Nakanishi, S. Fukushima, Y. Yamasaki, H. Koyama, N. Nishiyama and K. Kataoka, *J. Am. Chem. Soc.*, 2008, **130**, 16287.
- 23 D. Y. Chen, X. W. Xia, H. W. Gu, Q. F. Xu, J. F. Ge, Y. G. Li, N. J. Li and J. M. Lu, *J. Mater. Chem.*, 2011, **21**, 12682.
- 24 X. Mei, D. Y. Chen, N. J. Li, Q. F. Xu, J. F. Ge, H. Li, B. X. Yang, Y. J. Xu and J. M. Lu, *Soft Matter*, 2012, **8**, 5309.
- 25 G. Qi, Y. B. Wang, L. Estevez, A. K. Switzer, X. N. Duan, X. F. Yang and E. P. Giannelis, *Chem. Mater.*, 2010, **22**, 2693.
- 26 J. Park, K. An, Y. Hwang, J. G. Park, H. J. Noh, J. Y. Kim, J. H. Park, N. M. Hwang and T. Hyeon, *Nat. Mater.*, 2004, **3**, 891.
- 27 S. Perrier, P. Takolpuckdee and C. A. Mars, *Macromolecules*, 2005, **38**, 2033.
- 28 B. R. Kaafarani, B. Wex, F. Wang, O. Catanesu, L. C. Chien and D. C. Neckers, *J. Org. Chem.*, 2003, **68**, 5377.
- 29 N. Nasongkla, E. Bey, J. Ren, H. Ai, C. Khemtong, J. S. Guthi, S. F. Chin, A. D. Sherry, D. A. Boothman and J. Gao, *Nano Lett.*, 2006, **6**, 2427.
- 30 S. Perrier, P. Takolpuckdee and C. A. Mars, *Macromolecules*, 2005, **38**, 2033.
- 31 S. Dhar, Z. Liu, J. Thomale, H. Dai and S. J. Lippard, *J. Am. Chem. Soc.*, 2008, **130**, 11467.
- 32 Y. Gao, Y. Chen, X. F. Ji, X. Y. He, Q. Yin, Z. W. Zhang, J. L. Shi and Y. P. Li, *ACS Nano*, 2011, **5**, 9788.
- 33 C. Yan, J. K. Kepa, D. Siegel, I. J. Stratford and D. Ross, *Mol. Pharmacol.*, 2008, **74**, 1657.
- 34 E. S. Lee, K. T. Oh, D. Kim, Y. S. Youn and Y. H. Bae, *J. Controlled Release*, 2007, **123**, 19.
- 35 E. Climent, R. M. Manez, F. Sancenon, M. D. Marcos, J. Soto, A. M. Maquieira and P. Amoros, *Angew. Chem., Int. Ed.*, 2010, **49**, 7281.
- 36 Y. F. Zhu, J. L. Shi, W. H. Shen, X. P. Dong, J. W. Feng, M. L. Ruan and Y. S. Li, *Angew. Chem., Int. Ed.*, 2005, **44**, 5083.
- 37 D. Y. Chen, M. J. Jiang, N. J. Li, H. W. Gu, Q. F. Xu, J. F. Ge, X. W. Xia and J. M. Lu, *J. Mater. Chem.*, 2010, **20**, 6422.
- 38 J. Sudimack and R. J. Lee, *Adv. Drug Delivery Rev.*, 2000, **41**, 147.
- 39 X. Yang, S. Pilla, J. J. Grailer, D. A. Steeber, S. Gong, Y. Chen and G. Chen, *J. Mater. Chem.*, 2009, **19**, 5812.
- 40 T. K. Jain, M. A. Morales, S. K. Sahoo and D. L. Leslie, *Mol. Pharmaceutics*, 2005, **2**, 194.
- 41 H. Yuan, K. Luo, Y. Lai, Y. Pu, B. He, G. Wang, Y. Wu and Z. Gu, *Mol. Pharmaceutics*, 2010, **7**, 953.
- 42 J. Park, M. K. Yu, Y. Y. Jeong, J. W. Kim, K. Lee, V. N. Phan and S. Jon, *J. Mater. Chem.*, 2009, **19**, 6412.
- 43 S. Laurent, D. Forge, M. Port, A. Roch, C. Robic, L. V. Elst and R. N. Muller, *Chem. Rev.*, 2008, **108**, 2064.